

Received January 13, 2022, accepted February 26, 2022, date of publication March 2, 2022, date of current version March 17, 2022.

Digital Object Identifier 10.1109/ACCESS.2022.3156094

# Low Noise Balanced Homodyne Detector for Quantum Noise Measurement

SHUBO LANG<sup>1</sup>, SHICHENG ZHANG<sup>1</sup>, XIAOLIN LI<sup>1</sup>, YUEPING NIU<sup>1,2</sup>,  
AND SHANGQING GONG<sup>1,2</sup>

<sup>1</sup>School of Physics, East China University of Science and Technology, Shanghai 200237, China

<sup>2</sup>Shanghai Engineering Research Center of Hierarchical Nanomaterials, Shanghai 200237, China

Corresponding author: Shicheng Zhang (sczhang@ecust.edu.cn)

This work was supported in part by the National Natural Science Foundation of China under Grant 12034007, Grant 11874146, Grant 12004112, and Grant 61835013; in part by the Shanghai Sailing Program under Grant 20YF1410800; and in part by the Shanghai Natural Science Foundation under Grant 20ZR1414300.

**ABSTRACT** The research of quantum noise in the interaction of laser and atoms plays a critical role in quantum optical experiments. The measurement of quantum noise is mainly based on the balanced homodyne detection method. Here, we reported a balanced homodyne detector with low noise, high gain, and high common-mode rejection ratio (CMRR) at the wavelength of 795 nm. By optimizing the selection of components and printed circuit board (PCB) layout, a minimum electronic noise of  $-96.7$  dBm is obtained. Over the range of 1 MHz to 5 MHz, we get a flat CMRR above 59 dB and a linear gain regime, which can enable a shot noise measurement with the laser power of  $100 \mu\text{W}$ . The developed detector can be used in quantum coherent experiments with a weak probe laser of power down to tens of microwatts.

**INDEX TERMS** Quantum noise, balanced homodyne detector, low noise, electromagnetically induced transparency.

## I. INTRODUCTION

The measurement of quantum noise is a vital step of many quantum optical experiments, such as squeezed state detection [1], coherent state detection [2], and quantum storage [3]. Balanced homodyne detection is a general method to measure quantum noise [4]. The main parameters of the balanced homodyne detector (BHD) are indexed in three points: 1) low electronic noise; 2) high common-mode rejection ratio (CMRR); 3) flat amplification gain [5], [6]. The measurement of quantum noise is strongly limited by electronic noise and gain. To reduce the influence of the electronic noise on the measured value, the clearance between electronic noise and shot noise should typically be greater than 10 dB [7].

Usually, BHD is mainly applied in the near-infrared (NIR) band greater than  $1 \mu\text{m}$ , such as 1550 nm [8]–[11] and 1064 nm [12]–[15]. Alkali atoms such as Rubidium (Rb) are potentially excellent optical mediums for quantum optical experiments [16]–[18], and the common wavelengths are mainly 780 nm and 795 nm. However, as we know, there are very few research works of BHD for the Rb. Hansen and co-workers designed a pulsed BHD with a bandwidth of

about 1 MHz and a CMRR of 85 dB for time-domain quantum measurement [5]. Moreover, Kumar and co-workers designed a detector with a bandwidth of about 100 MHz and a CMRR of 52.4 dB for the measurement of quantum optical field quadrature values both in the continuous-wave and pulsed regime [6]. For quantum optical experiments [19]–[22], such as electromagnetically induced transparency (EIT), the measurement of quantum noise usually requires BHD with a bandwidth of several megahertz [16], [23] and high CMRR. Thus, a BHD that can measure the quantum noise of weak light at several megahertz is needed.

In this paper, we designed a BHD with low noise and high CMRR for the measurement of quantum noise in the range of 5 MHz. We use a pair of photodiodes with low noise and high responsivity to construct the BHD. The alternating current (AC) and direct current (DC) amplification branches are separated by a combination of a capacitor and two inductors. As a result, we obtain a high-performance BHD with the minimum electronic noise of about  $-96.7$  dBm at the analysis frequency of 1.4 MHz. The CMRR is higher than 59 dB within the range from 1 MHz to 5 MHz, and the maximum clearance between quantum noise and electronic noise is higher than 25 dB for a local laser at 1 mW. The BHD has the potential to measure quantum noise of weak

The associate editor coordinating the review of this manuscript and approving it for publication was Z. G. Zang<sup>1</sup>.

**TABLE 1.** Main parameters of five different PDs. PC20-7 is produced by first sensor (Germany). S3399, S3883, S5971 and S5973 are produced by Hamamatsu (Japan).

Photodiode	Responsivity $/(A \cdot W^{-1})$	Capacitance / pF
PC20-7	0.61	20
S3399	0.58	20
S3883	0.58	6
S5971	0.55	3
S5973	0.51	1.6

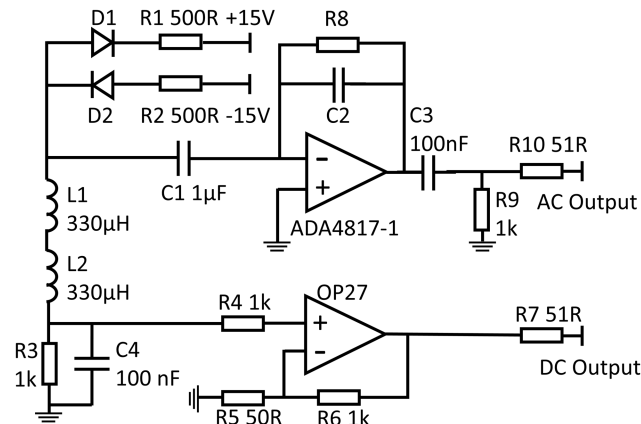


**FIGURE 1.** Diagram of the circuit principle. D1 and D2 are two photodiode (S5971). The DC flows through two inductors and is outputted via an in-phase proportional amplifier circuit constructed by a high precision operational amplifier OP27. The AC passes through capacitance C1 and then can be converted into a noise voltage signal by R8 through a transimpedance amplifier circuit constructed by broad bandwidth and low noise operational amplifier ADA4817-1.

probe laser with a power less than  $100 \mu W$  in quantum optical experiments.

## II. DESIGN OF THE BHD

Photodiode (PD) has a major contribution to the performance of BHD. Selecting PD which has high sensitivity, small junction capacitance, huge internal resistance, and low dark current can effectively decrease the electronic noise of BHD [24], [25]. By now, the selectable PDs for 795 nm are listed in TABLE 1 [26]. Consider the balance between the bandwidth and gain that we need, finally, we choose S5971 to construct our BHD. It has a high sensitivity ( $0.55 A/W$ ) at 795nm, a low junction capacitance (3 pF), and an ultra-low dark current (1 nA). Thus, it is very suitable for our requirements.

The diagram of the detector circuit is shown in Fig. 1. We built our detector by applying the self-subtraction photodetector scheme [27]. The DC flows through two inductors L1 and L2 to generate a voltage drop on the resistor R3. Resistor R3 and capacitance C4 form an RC low-pass filter to further filter the noise. Then, the DC section is output via an in-phase proportional amplifier circuit. The DC output is used to verify whether the laser is thoroughly received by each PD and meanwhile make sure the powers of the lasers injected into each PD are equal. The AC passes through the

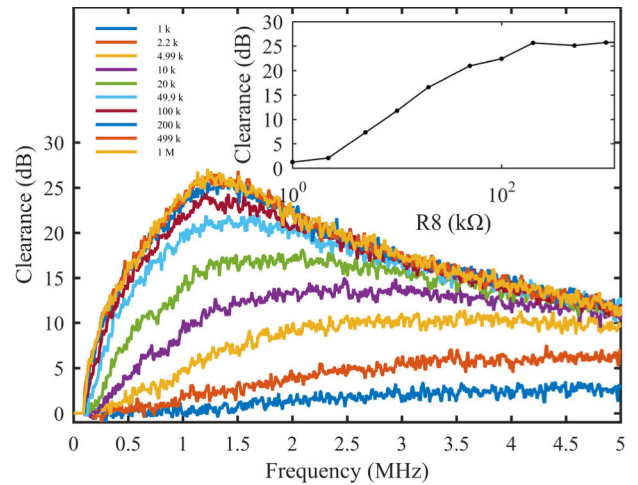


**FIGURE 2.** Clearance between quantum noise and electronic noise with different values of feedback resistance R8. The power of local light is 1mw. The inset shows clearance varies with R8 at an analysis frequency of 1.4 MHz.

capacitance C1 then is converted into a noise voltage signal by resistor R8. The noise power can be got by the AC output.

Transimpedance amplifier (TIA) is widely applied to convert the shot noise current to AC voltage [28]. We select ADA4817-1 as the operational amplifier of TIA. It has a low input current noise of  $2.5 fA/\sqrt{Hz}$  and an input bias current of 2 pA. The clearance between electronic noise and shot noise can be improved by selecting the appropriate feedback R8 and decoupling capacitor C2. Fig. 2 shows the clearance between quantum noise and electronic noise with different values of resistance R8 with a local light at 1 mW. The spectrum analyzer (SA) resolution bandwidth and video bandwidth are 30 kHz and 100 Hz respectively. We can see that as the feedback resistance R8 gradually increases from 1 kΩ to 200 kΩ, the clearance becomes progressively larger. After the resistance is greater than 200 kΩ, the clearance reaches saturation. Thus, we choose a 200 kΩ feedback resistor. To eliminate the self-excited oscillation effect, a decoupling capacitor with a value of 0.5 pF is applied.

To further reduce the electrical noise, the design of the printed circuit board (PCB) is an important factor [15]. A double-sided PCB is designed to minimize parasitic capacitances. All components are soldered on the surface layer of PCB and all tracks are kept as short as possible. As the upper layer of the PCB is mainly used as signal traces, the ground planes around the ADA4817-1, OP27, and the signal path are removed to minimize parasitic capacitances. The components should be placed along the direction of the signal. The power line should be far away from the signal line to avoid interference between the lines. The backside of the PCB is reserved as a whole ground plane to ensure that the analog ground level is consistent everywhere.

## III. EXPERIMENTAL SETUP AND RESULTS

To characterize the performance of the detector, we measured the electronic noise and CMRR. The experimental setup is

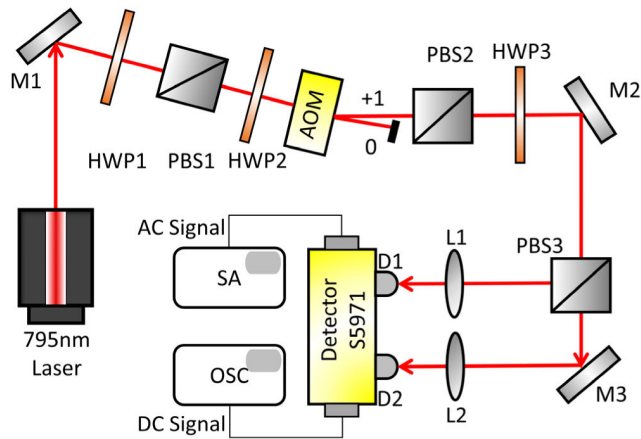


**FIGURE 3.** Schematic for measuring the electronic noise and CMRR of the detector. M: mirror; PBS: polarization beam splitter; AOM: acousto-optic modulator; D: S5971 PD; L: lens; SA: spectrum analyzer; OSC: digitizing oscilloscope. The AC and DC outputs are connected to the SA the OSC respectively.

shown in Fig. 3. The laser source is a 795 nm semiconductor laser and its amplitude can be modulated by the acoustic-optic modulator (AOM). CMRR is defined as the ratio of the power measured on one detector when the other is blocked by the power measured when both photodiodes are illuminated [12]. For the measurement of CMRR, the laser intensity received by the two PDs should be as equal as possible. Therefore, we use a combination of a half-wave plate (HWP3) and a polarization beam splitter (PBS3) to achieve it. The output beams from the PBS3 are injected into two PDs after being focused by two lenses with a focal length of 75 mm. By carefully adjusting the HWP3, we can get the maximum CMRR.

A typical result at the spectrum analyzer (Keysight N9020B) is shown in Fig. 4. The black curve is the internal noise of the spectrum analyzer (SA). The red curve is the measured electronic noise spectrum of the BHD in the absence of input laser. We can see that the minimum electronic noise is about  $-96.7$  dBm at the analysis frequency of 1.4 MHz. The blue curve indicates the noise spectrum of the unbalanced detector (one PD blocked, the other PD illuminated at the power of  $50 \mu\text{w}$ ) with a total power of  $100 \mu\text{w}$ . The peak at 1.4 MHz corresponds to the noise of the modulated signal on the amplitude modulator at  $-7.7$  dBm. The green curve corresponding to the differential mode signal shows the noise spectrum of the balanced detector (two PD illuminated at the power of  $50 \mu\text{w}$ , respectively). We can see that the CMRR is about 59 dB at 1.4 MHz. The insert shows that CMRR varies with analysis frequency. CMRR can keep a high value from about 1 MHz to 5 MHz. After the frequency is greater than 5 MHz, the CMRR starts to decrease.

In addition, to demonstrate the gain characteristics and bandwidth of the detector, we measured the shot noise of the BHD at different local oscillator powers, the results are shown in Fig. 5. To ensure the signal-to-noise ratio, the clearance between electronic noise and shot noise should typically be greater than 10 dB. Thus, the minimum power that can be detected is about  $100 \mu\text{w}$ . In particular, we can see the 3 dB

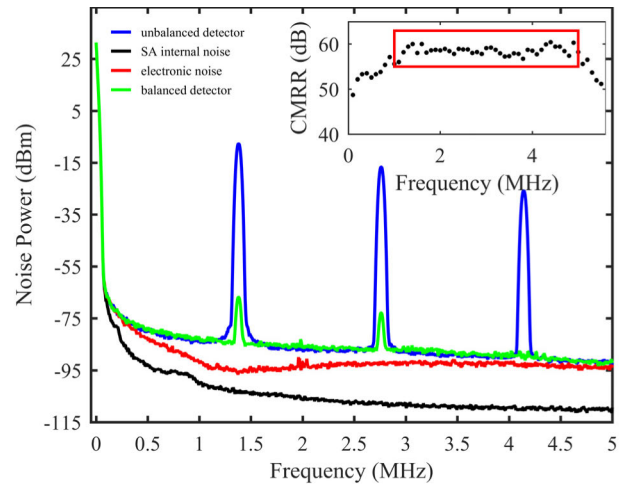


**FIGURE 4.** The electronic noise and CMRR of the detector with input power of  $100 \mu\text{w}$ . Black curve: the internal noise of SA. Red curve: the electronic noise spectrum of the BHD (two PDs blocked). Blue curve: the noise spectrum of the unbalanced detector (one PD blocked, the other PD illuminated). Green curve: the noise spectrum of the balanced detector (two PD illuminated). The insert shows that CMRR varies with analysis frequency.

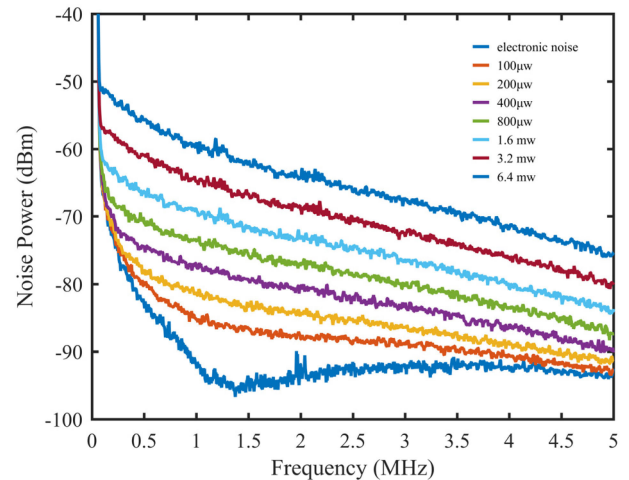


**FIGURE 5.** The shot noise of the BHD versus the analysis frequency at different local oscillator powers.

shift of the quantum noise trace with the local oscillator power double increased. This result can meet the requirements of many quantum optical experiments.

#### IV. APPLICATIONS

EIT is a typical quantum coherence phenomenon, and the quantum noise of EIT has been extensively researched [16], [18], [22], [23], [29], [30]. Near the resonance frequency, the strong control laser can induce a large noise to the probe laser. In the experiment of EIT, usually, the probe field needs to be very weak to avoid the nonlinear effect, and the typical power is about tens of microwatts. Limited to the electronic noise, in the current quantum noise experiment, the probe field power needs to be about one hundred microwatts to achieve a good signal-to-noise ratio (SNR) [16], [23].

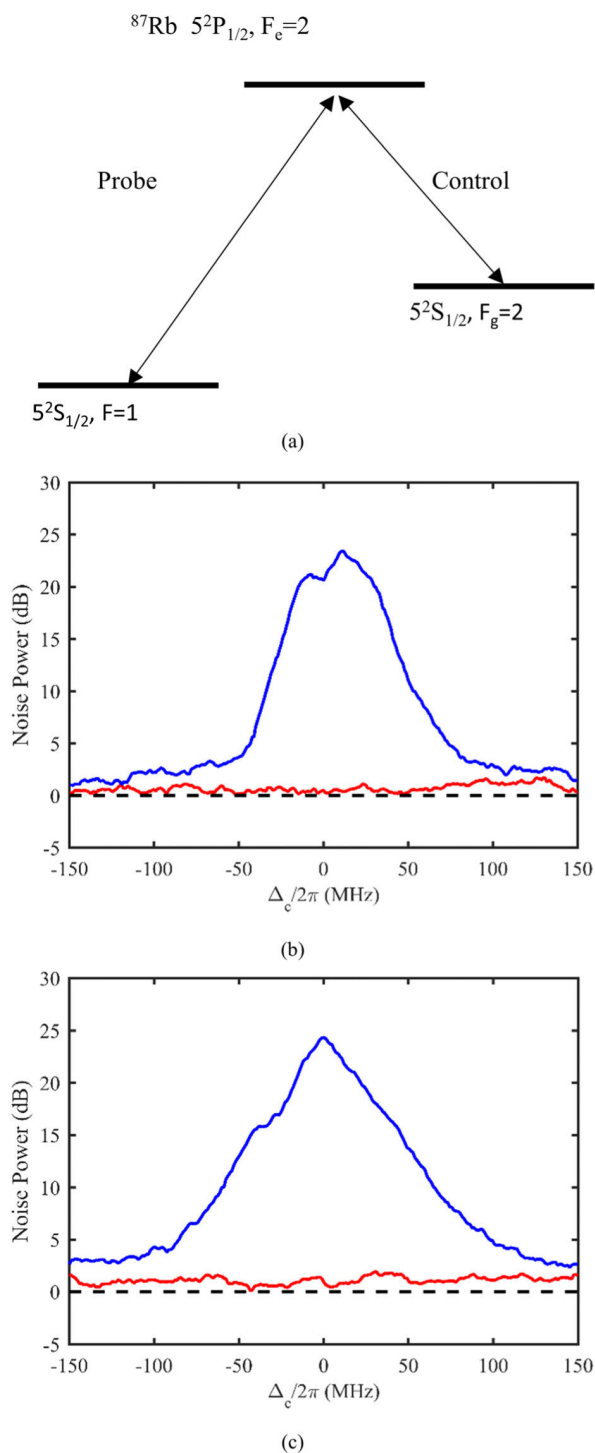


**FIGURE 6.** (a) The level structure of three-level atoms. (b) Amplitude noise spectra of the probe field. The relative phase between the local laser and the probe laser is 0. (c) Relative phase between the local laser and the probe laser is  $\pi/2$ . The black curve for the shot-noise limit. The blue curve for noise spectra with control laser and red curve for noise spectra without control laser.

Here, we use the homemade detector to carry out an experimental measurement of EIT quantum noise. Figure. 6a shows the energy-level structure. The probe field is supplied by a diode laser with a wavelength of 795 nm, and the frequency is

tuned to be resonant with the transition of  $|5^2S_{1/2}, F = 1 \rangle \rightarrow |5^2P_{1/2}, F = 2 \rangle$ . The control field is supplied by another diode laser with a wavelength of 795 nm, and it is tuned to scan near the transition of  $|5^2S_{1/2}, F = 2 \rangle \rightarrow |5^2P_{1/2}, F = 2 \rangle$ . We use the balanced homodyne detection method to measure the quantum noise. The power of control, probe, and local fields are 30 mW, 10  $\mu\text{W}$ , and 350  $\mu\text{W}$ , respectively. Figure. 6b and 6c are the measured amplitude noise spectra of the probe field with different relative phases between the control and probe fields, see the blue curves. The black curves are the shot-noise limit, and the red curves are the noise spectra without the control field. When the relative phase is zero, the noise is converted from control light. When the relative phase is  $\pi/2$ , the noise not only includes the part converted from the control field but also those converted from the phase noise of the probe field itself. We can see that, even when the probe field power is down to 10  $\mu\text{W}$ , the noise spectrum still has a good SNR.

## V. CONCLUSION

We have developed a balanced homodyne detector with low noise, high gain, and high CMRR by using a pair of photodiodes with low noise and high responsivity at 795 nm. The AC and DC amplification branches are separated with the assistant of a capacitor and two inductors. By optimizing the selection of components and PCB layout, we achieved a significant reduction in electronic noise. As a result, a minimum electronic noise of  $-96.7$  dBm is achieved, which allows us to measure the shot noise of a weak laser with a power of 100  $\mu\text{W}$ . The CMRR of the detector can reach 59 dB in the frequency range from 1 MHz to 5 MHz, so it's suitable for the measurement of quantum noise of quantum optical experiments. We observed a 3dB shift of the quantum noise trace when the laser power increases to twice, indicating that the detector has a linear response over the measurement regime. The low-noise detector can help us to measure the quantum noise characteristics of EIT even when the probe field power is down to 10  $\mu\text{W}$ . We believe the detector can have wide applications in practical quantum optical experiments.

## REFERENCES

- [1] X. D. Yu, W. Li, S. Y. Zhu, and J. Zhang, "Mach-Zehnder interferometer with squeezed and EPR entangled optical fields," *Chin. Phys. B*, vol. 25, no. 2, 2016, Art. no. 020304.
- [2] S. F. Pereira, M. Xiao, H. J. Kimble, and J. L. Hall, "Generation of squeezed light by intracavity frequency doubling," *Phys. Rev. A, Gen. Phys.*, vol. 38, no. 9, pp. 4931–4934, Nov. 1988.
- [3] A. Kuzmich, K. Mølmer, and E. S. Polzik, "Spin squeezing in an ensemble of atoms illuminated with squeezed light," *Phys. Rev. Lett.*, vol. 79, no. 24, pp. 4782–4785, Dec. 1997.
- [4] H. P. Yuen and V. W. S. Chan, "Noise in homodyne and heterodyne detection," *Opt. Lett.*, vol. 8, no. 3, pp. 177–179, 1983.
- [5] H. Hansen, T. Aichele, C. Hettich, P. Lodahl, A. I. Lvovsky, J. Mlynek, and S. Schiller, "Ultrasensitive pulsed, balanced homodyne detector: Application to time-domain quantum measurements," *Opt. Lett.*, vol. 26, no. 21, pp. 1714–1716, Nov. 2001.
- [6] R. Kumar, E. Barrios, A. MacRae, E. Cairns, E. H. Huntington, and A. I. Lvovsky, "Versatile wideband balanced detector for quantum optical homodyne tomography," *Opt. Commun.*, vol. 285, no. 24, pp. 5259–5267, Nov. 2012.



- [7] M. B. Gray, D. A. Shaddock, C. C. Harb, and H.-A. Bachor, "Photodetector designs for low-noise, broadband, and high-power applications," *Rev. Sci. Instrum.*, vol. 69, no. 11, pp. 3755–3762, Nov. 1998.
- [8] Y.-M. Chi, B. Qi, W. Zhu, L. Qian, H.-K. Lo, S.-H. Youn, A. I. Lvovsky, and L. Tian, "A balanced homodyne detector for high-rate Gaussian-modulated coherent-state quantum key distribution," *New J. Phys.*, vol. 13, no. 1, Jan. 2011, Art. no. 013003.
- [9] D. Huang, J. Fang, C. Wang, P. Huang, and G.-H. Zeng, "A 300-MHz bandwidth balanced homodyne detector for continuous variable quantum key distribution," *Chin. Phys. Lett.*, vol. 30, no. 11, Nov. 2013, Art. no. 114209.
- [10] B. Qi, L.-L. Huang, L. Qian, and H.-K. Lo, "Experimental study on the Gaussian-modulated coherent-state quantum key distribution over standard telecommunication fibers," *Phys. Rev. A, Gen. Phys.*, vol. 76, no. 5, Nov. 2007, Art. no. 052323.
- [11] X. Zhang, Y. Zhang, Z. Li, S. Yu, and H. Guo, "1.2-GHz balanced homodyne detector for continuous-variable quantum information technology," *IEEE Photon. J.*, vol. 10, no. 5, pp. 1–10, Oct. 2018.
- [12] X. Jin, J. Su, Y. Zheng, C. Chen, W. Wang, and K. Peng, "Balanced homodyne detection with high common mode rejection ratio based on parameter compensation of two arbitrary photodiodes," *Opt. Exp.*, vol. 23, no. 18, p. 23859, Sep. 2015.
- [13] R. Okubo, M. Hirano, Y. Zhang, and T. Hirano, "Pulse-resolved measurement of quadrature phase amplitudes of squeezed pulse trains at a repetition rate of 76 MHz," *Opt. Lett.*, vol. 33, no. 13, pp. 1458–1460, Jul. 2008.
- [14] J. R. Wang, Q. W. Wang, L. Tian, J. Su, and Y. H. Zheng, "A low-noise, high-SNR balanced homodyne detector for the bright squeezed state measurement in 1–100 kHz range," *Chin. Phys. B*, vol. 29, Jan. 2020, Art. no. 034205.
- [15] H. Zhou, W. Wang, C. Chen, and Y. Zheng, "A low-noise, large-dynamic-range-enhanced amplifier based on JFET buffering input and JFET bootstrap structure," *IEEE Sensors J.*, vol. 15, no. 4, pp. 2101–2105, Apr. 2015.
- [16] F. Wang, X. D. Yu, Z. M. Meng, and J. Zhang, "Experimental study of quantum noise characteristics of the probe field in electromagnetically induced transparency medium," *Acta Optica Sinica*, vol. 34, no. 5, 2014, Art. no. 0527001.
- [17] Y. Xiao, T. Wang, M. Baryakhtar, M. Van Camp, M. Crescimanno, M. Hohensee, L. Jiang, D. F. Phillips, M. D. Lukin, S. F. Yelin, and R. L. Walsworth, "Electromagnetically induced transparency with noisy lasers," *Phys. Rev. A, Gen. Phys.*, vol. 80, no. 4, Oct. 2009, Art. no. 041805.
- [18] M. T. L. Hsu, G. Hétet, O. Glöckl, J. J. Longdell, B. C. Buchler, H.-A. Bachor, and P. K. Lam, "Quantum study of information delay in electromagnetically induced transparency," *Phys. Rev. Lett.*, vol. 97, no. 18, Nov. 2006, Art. no. 183601.
- [19] M. Fleischhauer and M. D. Lukin, "Dark-state polaritons in electromagnetically induced transparency," *Phys. Rev. Lett.*, vol. 84, no. 22, pp. 5094–5097, May 2000.
- [20] K.-J. Boller, A. Imamoglu, and S. E. Harris, "Observation of electromagnetically induced transparency," *Phys. Rev. Lett.*, vol. 66, no. 20, pp. 2593–2596, May 1991.
- [21] C. Liu, Z. Dutton, C. H. Behroozi, and L. V. Hau, "Observation of coherent optical information storage in an atomic medium using halted light pulses," *Nature*, vol. 409, pp. 490–493, Jan. 2001.
- [22] J. Zhang, J. Cai, Y. Bai, J. Gao, and S.-Y. Zhu, "Optimization of the noise property of delayed light in electromagnetically induced transparency," *Phys. Rev. A, Gen. Phys.*, vol. 76, no. 3, Sep. 2007, Art. no. 033814.
- [23] Y. Li, "The quantum noise properties of light field in electromagnetically induced transparency media," Ph.D. dissertation, Dept. Opto. Elect., Shanxi Univ., Shanxi, China, 2013.
- [24] J. Xue, "Measurement of vacuum quantum noise at low frequencies," M.S. thesis, Dept. Opto. Elect., Shanxi Univ., Shanxi, China, 2016.
- [25] S. Wang, X. Xiang, C. Zhou, Y. Zhai, R. Quan, M. Wang, F. Hou, S. Zhang, R. Dong, and T. Liu, "Simulation of high SNR photodetector with L-C coupling and transimpedance amplifier circuit and its verification," *Rev. Sci. Instrum.*, vol. 88, no. 1, Jan. 2017, Art. no. 013107.
- [26] L. X. Ma, J. L. Qin, Z. H. Yan, and X. J. Jia, "Fast response balanced homodyne detector for continuous-variable quantum memory," *Acta Optica Sinica*, vol. 38, no. 2, 2018, Art. no. 0227001.
- [27] X. L. Jin, "Study on control and detection systems for squeezed state of light with continuous variable," Ph.D. dissertation, Dept. Opto. Elect., Shanxi Univ., Shanxi, China, 2016.
- [28] H. Zhou, W. Yang, Z. Li, X. Li, and Y. Zheng, "A bootstrapped, low-noise, and high-gain photodetector for shot noise measurement," *Rev. Sci. Instrum.*, vol. 85, no. 1, Jan. 2014, Art. no. 013111.
- [29] A. Dantan, A. Bramati, and M. Pinard, "Atomic quantum memory: Cavity versus single-pass schemes," *Phys. Rev. A, Gen. Phys.*, vol. 71, no. 4, Apr. 2005, Art. no. 043801.
- [30] A. Peng, M. Johnsson, W. P. Bowen, P. K. Lam, H.-A. Bachor, and J. J. Hope, "Squeezing and entanglement delay using slow light," *Phys. Rev. A, Gen. Phys.*, vol. 71, no. 3, Mar. 2005, Art. no. 033809.



**SHUBO LANG** received the B.S. degree in opto-electronic information science and engineering from the East China University of Science and Technology, Shanghai, China, in 2019, where he is currently pursuing the M.S. degree in physics.

His research interests include balanced homodyne detector, electromagnetically induced transparency, and quantum noise measurement.



**SHICHENG ZHANG** received the Ph.D. degree from the East China University of Science and Technology, Shanghai, China, in 2019.

He is currently a Distinguished Associate Research Fellow with the School of Physics, East China University of Science and Technology. His current research interests include quantum noise measurement and electromagnetically induced transparency.



**XIAOLIN LI** received the Ph.D. degree in optics from the Shanghai Institute of Optics and Fine Mechanics, Chinese Academy of Sciences, China, in 2007.

He is currently a Researcher with the School of Physics, East China University of Science and Technology, China. His current research interests include quantum metrology and quantum optics.



**YUEPING NIU** was born in 1977. She received the Ph.D. degree from the Shanghai Institute of Optics and Fine Mechanics, Chinese Academy of Sciences, China, in 2006.

She is currently a Professor with the School of Physics, East China University of Science and Technology, China. Her current research interests include nonlinear enhancement, ultrashort laser pulse, and quantum interference.



**SHANGQING GONG** was born in 1963. He received the Ph.D. degree from the Institute of Physics, Chinese Academy of Sciences, China, in 1992.

He is currently a Professor with the School of Physics, East China University of Science and Technology, China. His current research interests include quantum interference, nonlinear optics, and cavity induced transparency.